# Dalton Transactions

## Accepted Manuscript

This article can be cited before page numbers have been issued, to do this please use: S. Mukhopadhyay, M. Saha, M. Das, R. Nasani, I. Choudhuri, M. M. Shaikh, B. Pathak, M. Yousufuddin and H. P. Nayek, *Dalton Trans.*, 2015, DOI: 10.1039/C5DT01471A.




ROYAL SOCIETY OF CHEMISTRY

www.rsc.org/dalton

View Article Online
DOI: 10.1039/C5DT01471A



# Targeted Water Soluble Copper-tetrazolate Complexes : Interactions with Biomolecules and Catecholase like Activities

Manideepa Saha,[a] Mriganka Das,[a] Rajendar Nasani,[a] Indrani Choudhuri,[a] Muhammed Yousufuddin,[b] Hari Pada Nayek,[c] Mobin M Shaikh,[a] Biswarup Pathak,[a] Suman Mukhopadhyay*[a]

[a]*Department of Chemistry, School of Basic Sciences, Indian Institute of Technology Indore, IET-DAVV Campus, Khandwa Road, Indore 452017, India. Tel : +91 731 2438 705 Fax: +91 731 2361 482 E-mail: suman@iiti.ac.in*

[b]*University of North Texas at Dallas, Life and Health Sciences Department,7400 University Hills Blvd, 300 Founder's Hall, Dallas, TX 75241, USA.*

[c]*Department of Applied Chemistry, Indian School of Mines, Dhanbad, 826004, Jharkhand, India, E-mail:*

## Abstract

Two new mononuclear water soluble copper (II) complexes [Cu{(5-pyrazinyl)tetrazolate}$_2$(1,10-phenanthroline)] **1** and [Cu{(5-pyrazinyl)tetrazolate}(1,10-phenanthroline)$_2$]$(NO_3)_{0.5}(N_3)_{0.5}$ **2** have been synthesized using the metal mediated [2 + 3] cycloaddition reaction between copper bound azide and pyrazinecarbonitrile. The interaction of these copper tetrazolate complexes **1** and **2** with biomolecules like DNA and bovine serum albumin (BSA) are studied and catecholase like catalytic activity of compound **2** is also explored. Structural determination reveals that both compounds **1** and **2** are octahedral in nature. Screening tests were conducted to quantify the binding ability of complexes (**1** and **2**) towards DNA and it was revealed that complex **2** has a stronger affinity to bind towards CT-DNA. DFT studies indicated that a lower HOMO-LUMO energy gap between the DNA fragment and metal complexes might be the reason for this type of stronger interaction. DNA cleavage activity was explored through gel-electrophoresis and moderate to strong DNA cleavage property was observed in the presence and absence of co-reagents. Inhibition of cleavage in the presence of sodium azide indicates the propagation of the activity through production of singlet molecular oxygen. Furthermore enzyme kinetic studies reflect that

View Article Online
DOI: 10.1039/C5DT01471A

complex **2** is also effective in mimicking catecholase like activities. ESI-MS spectral study indicates probable involvement of dimeric species $[(phen)_2Cu\text{-}(OH)_2\text{-}Cu(phen)_2]^{2+}$ in the catalytic cycle.

## Introduction

Interactions of various 5-substituted tetrazoles with copper ions have been widely investigated by different researchers in the past few years.[1-14] However, the prime focus of these kinds of studies remain limited to generation of metal-organic frameworks, where the tetrazole ligand is able to participate in nine different types of coordination, with a vast array of structural diversities having various topologies. Solvothermal synthesis of copper-tetrazolate complexes mostly have taken control in the arena of generation of polymeric materials.[1,4,6,7] Some of these synthesized frameworks or mononuclear compounds have shown interesting magnetic,[1,6,7,11,13] catalytic,[2] photoluminescence[5,6] or gas absorption[3,8,12] properties.

The binding of DNA with tetrazolo metal complexes has attracted much attention recently because of their site specific binding properties and wide range of applications. The interaction between DNA and copper tetrazolate complex are relatively rare in literature,[15] however to the best of our knowledge the interaction of copper-tetrazolate complexes with bovine serum albumin (BSA) or any kind of bioinspired catalytic activities of these complexes have not been explored yet. The rational reasoning might be lying in the fact that the solvothermally generated uncontrolled copper-tetrazolate frameworks are mostly insoluble in nature that make them unsuitable for this kind of investigation. However, as per our continuous endeavor to generate metal tetrazolate complexes in a more controlled and environmental friendly condition, herein we report the synthesis and structural characterization of mononuclear copper tetrazolate complexes [Cu{(5-pyrazinyl)tetrazolate}$_2$(1,10-phenanthroline)] **1** and [Cu{(5-pyrazinyl)tetrazolate}(1,10-phenanthroline)$_2$]$(NO_3)_{0.5}(N_3)_{0.5}$ **2**. Both the complexes **1** and **2** exhibit interesting interactions with biomolecules like DNA and serum albumin protein. Furthermore, compound **2** has shown interesting catecholase like activity which is also reported here. Interaction of the complexes with DNA are further investigated with Density functional theory.

View Article Online
DOI: 10.1039/C5DT01471A



## Results and Discussion

To tackle the problem of lower solubility of copper-tetrazolate complex and to explore the possibilities in the domain of interaction with biomolecules, pyrazinecarbonitrile was chosen as a prospective precursor of tetrazolate ligand with extra hydrogen bonding site in the form of pyrazinyl nitrogen. A copper azide polymer complex $[Cu(phen)(N_3)_2]_n$ was chosen as the starting material where the ratio between copper to azide was 1:2 inducing the possibility for cycloaddition with two molecules to pyrazine nitrile to generate two chelating bidentate 5-pyrazinyltetrazole ligands which along with one ancilliary 1,10-phenanthroline ligand completes the octahedral geometry surrounding the copper center and helps to break down the polymeric complex to a monomeric entity. Reaction between $[Cu(phen)(N_3)_2]_n$ and excess of pyrazine carbonitrile in DMF at refluxing condition provides a mixture of compound **1** and **2** upon addition of $NaNO_3$. ESI-MS indicates the presence of two separate species viz. $[Cu(phen)(pzta)_2]$ **1** and $[Cu(phen)_2(pzta)]^+$ **2** [phen = 1,10-phenanthroline and pzta = 5-pyrazinyltetrazolate] (Scheme 1 & Figure 1). The cationic complex **2** was solidified upon addition of $NaNO_3$ as $[Cu\{(5\text{-pyrazinyl})tetrazolate\}(1,10\text{-phenanthroline})_2](NO_3)_{0.5}(N_3)_{0.5}$ **2** (scheme 1). The mixture of compounds **1** and **2** were further separated by cation-exchange chromatography using SP-Sephadex C25. The neutral complex **1** was obtained by eluting with methanol where as the cationic complex **2** was isolated by elution with aqueous 0.1 M $NaNO_3$ solution. The compound **2** was also prepared through different method which provides $[Cu\{(5\text{-pyrazinyl})tetrazolate\}(1,10\text{-phenanthroline})_2](NO_3)_{0.5}(N_3)_{0.5}$ **2** as the exclusive product only. The [2 + 3] dipolar cycloaddition reaction between copper ligated azide $[Cu(phen)_2N_3](NO_3)$ with pyrazine carbonitrile under refluxing condition in DMF yielded a green residue upon concentration. This residue was dissolved in acetonitrile and layered with diethylether to obtain a relatively small amount of green coloured crystals, which were physically separated. Those crystals were then dissolved in acetonitrile and layered with ether. This procedure was repeated several times to obtain an increasingly more pure compound **2** and the remaining mother solution was rejected. Both the compounds ( **1** and **2**) were characterized by IR, ESI-MS spectroscopy, elemental analyses and single crystal X-ray diffraction method.

View Article Online
DOI: 10.1039/C5DT01471A



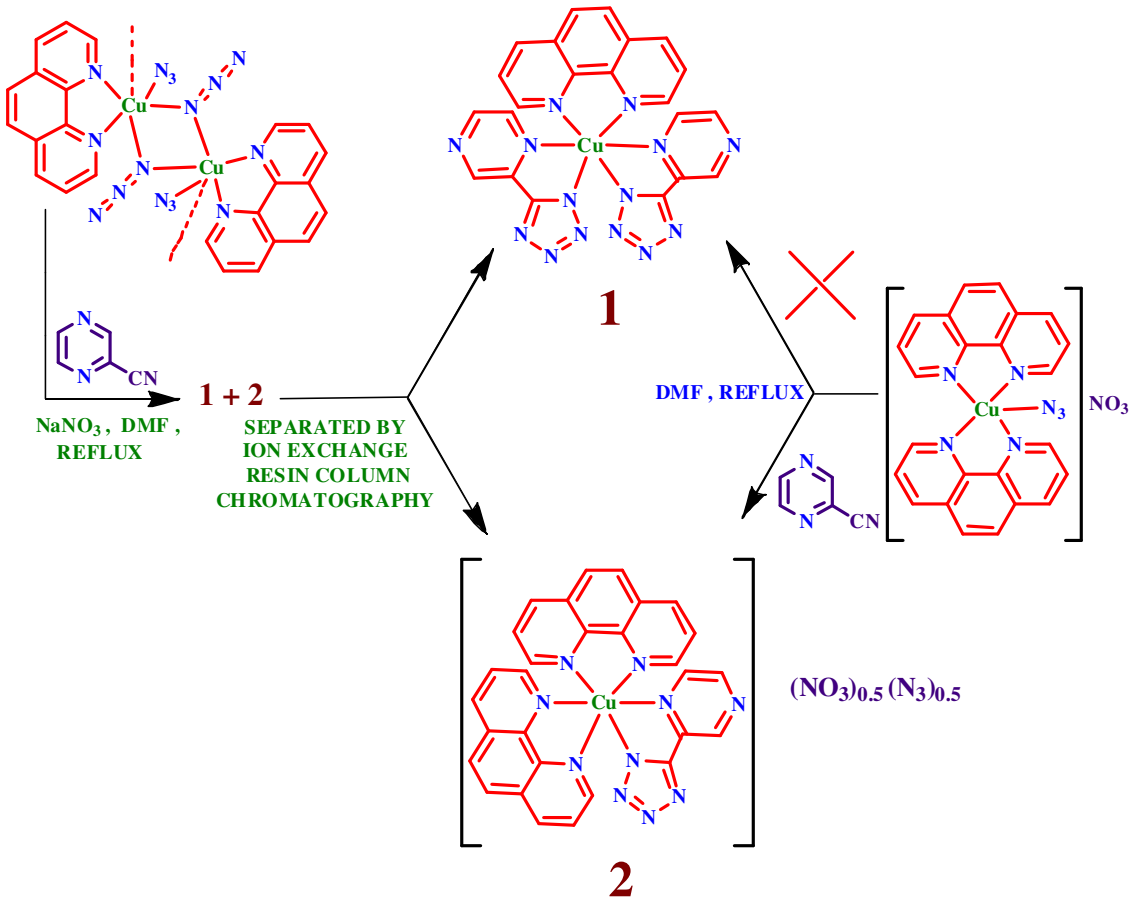


**Scheme 1. Schematic representation for the synthesis of complex [Cu(phen)(pzta)$_2$] 1 and** [Cu{(5-pyrazinyl)tetrazolate}(1,10-phenanthroline)$_2$] $(NO_3)_{0.5}(N_3)_{0.5}$ **2.**

View Article Online
DOI: 10.1039/C5DT01471A



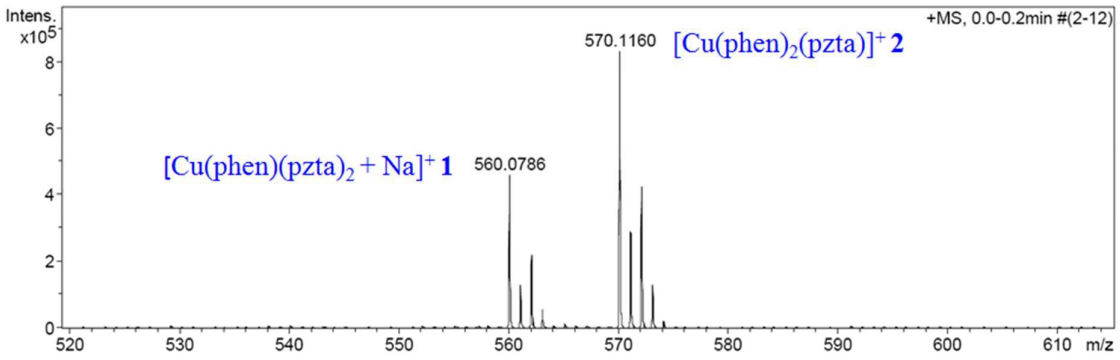


**Figure 1:** ESI-MS shows the presence of two separate species viz. $[Cu(phen)(pzta)_2 + Na]^+$ **1** and $[Cu(phen)_2(pzta)]^+$ **2** [phen = 1,10-phenanthroline and pzta = 5-pyrazinyltetrazolate]

Compound **1** shows a typical band at 1681 $cm^{-1}$ for tetrazolate ligand instead of two bands around 2057 $cm^{-1}$ for ligated azide in starting compound.[16] Compound **2** also confirms the presence of free azide, tetrazolate and nitrate ion through their signature bands at 2111 $cm^{-1}$ , 1628 $cm^{-1}$ and 1377 $cm^{-1}$ in IR spectrum, respectively.[17] The ESI-MS spectrum for the mixture of compounds shows two main peaks at 570.116 and 560.0786 corresponding to the cationic complex of $[Cu(phen)_2(pzta)]^+$ **2** and molecular ion peak of $[Cu(phen)(pzta)_2 + Na]^+$ **1**, respectively (Figure 1). However after separation of the mixtures, the respective pure compounds were further characterized through ESI-MS spectra (as shown in Figure S1 for complex **1** and Figure S2 for complex **2**). As the compounds **1** and **2** obtained show good solubility in common polar solvents including water, we were tempted to check their interaction with different biomolecules and explore the catecholase like activity since these areas are relatively unexplored for copper tetrazolate complexes.

The exact structures of the copper complexes were determined by single crystal X-ray crystallographic study. Compound **1** crystallizes in the space group P-1 (Table 1) and displays two molecules with very similar geometries (Figure 2). The central ion is situated in the distorted octahedral environment where both the tetrazole ligands act as chelating bidentate fashion (Figure 2). The N-Cu-N bond angle in tetrazole ligands are found to be in the range of 72-74° (Table 2), because of the very small bite. The Cu-N bond distances are found to be within the expected range except the pyrazinyl nitrogen which are coordinated axially and making distance around 2.4-2.5 Å, because of Jahn-Teller distortion.[18]

View Article Online
DOI: 10.1039/C5DT01471A



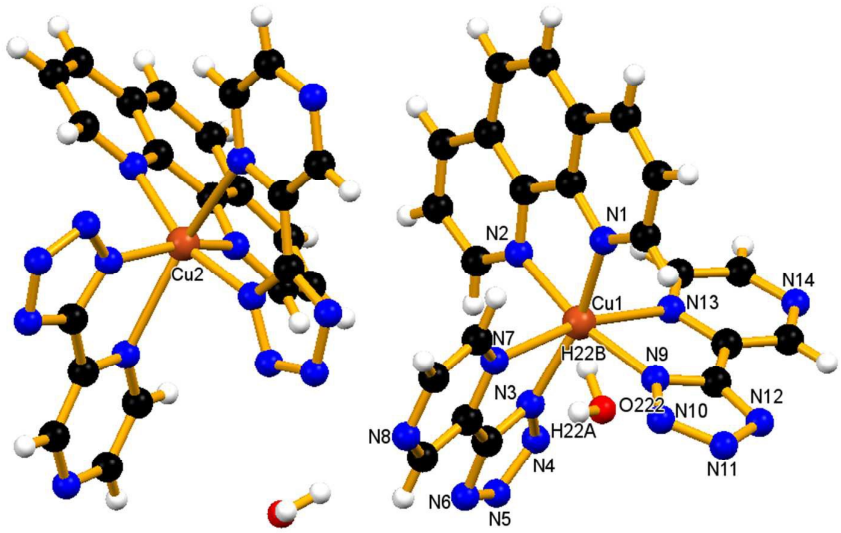


**Figure 2:** Molecular structure of $[Cu(phen)(pzta)_2](H_2O)$ **1** with the atomic numbering scheme.

Compound **2** crystallizes in the space group P-1 with one Cu complex, one-half azide, and one-half nitrate in the asymmetric unit for a Z value of 2 (Figure S3). The azide and nitrate sit on inversion centers and are disordered. The disorder was treated with ISOR restraints. The central atom exists in the center of a highly distorted octahedral geometry and crystallizes in the space group P-1 (Table 1). The pyrazine nitrogen is found to be coordinated to the metal center at a distance of 2.678 Å generating a semi-coordinated bond (Table 3).[19] Moreover, the small bite angle of the tetrazole ligand (70.8°) makes the molecule further distorted (Table 2). The nitrate and azide counterion are further enjoined with each other through complicated hydrogen bonding to form a three dimensional hydrogen bonded network (Figure S4).

The crystal structure of complex **2** contains two disordered water molecules which could not be modeled by discrete atoms. Their contribution was subtracted from the diffraction pattern by the "SQUEEZE" method.

To ascertain the number of water molecules in the complex thermogravimetric analysis was carried out. Complex 2 shows first weight loss of 5% within the range of 25-70 °C (Figure S5). This corresponds to the loss of four molecules of water of crystallization for one unit cell.

View Article Online
DOI: 10.1039/C5DT01471A



The electronic absorption spectra for both the complexes were recorded in methanol. Complex **1** reveals a shoulder around 660 nm and a low intensity peak for complex **2** was observed at 662 nm, characteristic of d-d transition band arising due to $^2B_{1g} \rightarrow {}^2E_g$ transition of tetragonally distorted octahedral geometry.[20] The presence of other electronic transitions which appear in the UV region can be correlated to the $\pi \rightarrow \pi^*$ transition in the ligand (Table 4).[21]

To explore the possibility of these copper complexes binding with CT-DNA (which has been found to be a critical step for the chemical nuclease activities of metal complexes) DNA was added over several steps with increasing amounts while changes in the absorption spectrum of the metal complex were monitored. It has been reported that interaction between metal complexes and DNA bases may lead to intercalation where hypochromic shift in the UV region was found to be a manifestation of that phenomena.[22,23] Furthermore a bathochromic shift indicates the decrease in the energy gap between the highest occupied and lowest unoccupied molecular orbital when the complex binds to DNA.[24] Absorption spectral titration carried out for compounds **1** and **2** reveals a decrease in molar absorptivity with a slight bathochromic shift indicating a possible interaction between aromatic moieties of the complex with DNA base pairs and stabilization of CT-DNA duplex. In the presence of DNA, complex **1** exhibited hypochromism of 10% at 275 nm (Figure S6) where as for complex **2** it increased to 20% (Figure S7), revealing considerable interaction between complexes and DNA. These interactions are attributed to $\pi \rightarrow \pi^*$ transition of the complex. The hypochromicity and bathochromic shift indicates the intercalative mode of binding and considerable stacking interaction between aromatic chromophore and base pairs of DNA. The plot of $[DNA]/[\varepsilon_a - \varepsilon_f]$ versus [DNA] (where $\varepsilon_a = A_{obs}/[compound]$ and extinction coefficient of the free compound) gives a straight line and the ratio of the slope to the intercept gives the intrinsic binding constant $K_b$. The values of the intrinsic binding constant for **1** (Figure S8) and **2** (Figure S9) were found to be 2.02 X $10^4$ $M^{-1}$ and 2.88 X $10^4$ $M^{-1}$ respectively. These values are moderate in nature with respect to the other ternary copper complexes reported so far. [25]

View Article Online
DOI: 10.1039/C5DT01471A



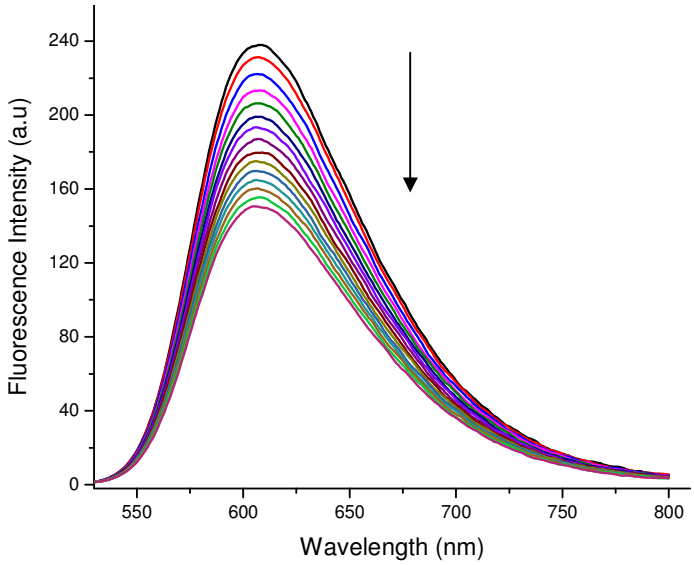


**Figure 3:** ETBr displacement assay by change in fluorescent intensity of EB with respect to conc.of complex **1**.

To order to obtain further information and investigate the interaction mode between the complex and CT-DNA, fluorescence titration experiments were carried out using ethidium bromide (EB) as a spectral probe. EB shows reduced emission intensity in buffer because of significant solvent quenching, however in presence of CT-DNA the emission intensity gets enhanced because of intercalative binding of EB to DNA. In presence of metal complex which competes with EB to bind the DNA a noteworthy reduction of emission intensity are generally observed.[24] In our experiment the fluorescence intensity at 607 nm showed significant decreasing trend with increasing concentration of complex **1** (Figure 3) and **2** (Figure 4) due to the displacement of DNA bound EB by copper complex. The $K_q$ value which was obtained from Stern-Volmer plot was found to be 4.18 X $10^3$ $M^{-1}$and 3.30 X $10^4$ $M^{-1}$ for complex **1** (Figure S10) and **2** (Figure S11), respectively. This shows a greater

View Article Online
DOI: 10.1039/C5DT01471A

interaction for compound **2** over compound **1**. The corresponding $K_b$ values obtained from the Scatchard plot (Figure S12 and Figure S13) where found to be 1.27 X $10^4$ $M^{-1}$ and 1.73 X $10^5$ $M^{-1}$, respectively. The values obtained are consistent with other values reported for similar copper complexes.[26,27]

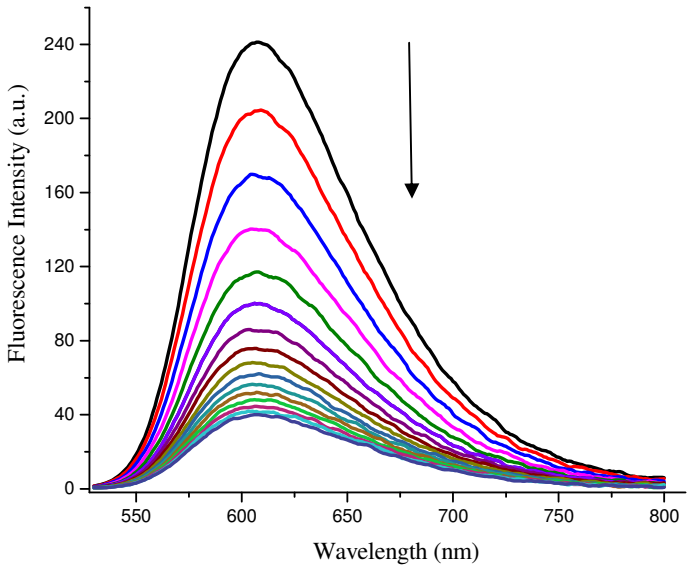


**Figure 4:** ETBr displacement assay by change in fluorescent intensity of EB with respect to conc. of complex **2**.

**DFT Study**:

In order to understand the DNA binding with the octahedral Cu-complexes (**1** and **2**), we have performed the density functional theory (DFT) study to investigate the role of the frontier orbitals towards such binding. The DNA structure is modelled as a deoxy-guanosine monophosphate (dGMP)[28] unit where one of the phosphate oxygen is methylated. Therefore, the total charge of the dGMP unit is negative. All the calculations are carried out in water solvent using B3LYP level of theory as implemented in the Gaussians 09 package.[29] The 6-311++G** basis set is used for the main group elements (C, N, O, P, and H) and LANL2DZ ECP basis set is used for Cu.[30,31] The solvent calculations are carried out using the polarizable continuum model[32] as implemented in the Gaussian 09.

View Article Online
DOI: 10.1039/C5DT01471A



The optimized Cu complexes (**1**, **2**) and dGMP structures are presented in S14. We have done the time dependent density functional theory (TDDFT) study[33-39] on the Cu complexes to understand their absorption spectrum. Our calculated results (Figure 5) show that the complex **1** and **2** absorbs at 288.38 nm and 296.31 nm respectively. The oscillator strength and expansion coefficients calculated for these two transitions are 0.057 and 0.68 for complex **1** and 0.031 and 0.36 for complex **2** respectively. The calculated values are very much in agreement with the experimental absorption spectra of the metal complexes. Our molecular orbital study shows that such transition corresponds to the ligand to metal charge transfer (LMCT) transition (Figure 5), which agrees well with our experimental findings.

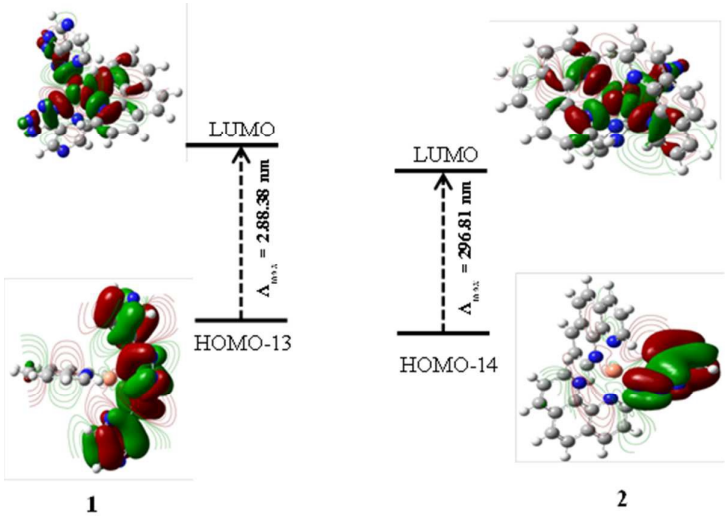


**Figure 5:** The calculated absorption ($\lambda_{max}$) corresponds to the LMCT of the Cu-complexes.

We have studied the frontier orbitals (Figure 6) of the dGMP and the Cu-complexes (**1** and **2**) to understand their role towards the binding. It is well established that the HOMO of the DNA fragments donate electron to the LUMO of the metal complexes.[40,41] So, we have calculated and presented (Figure 6) the HOMO energy of the dGMP structure with respect to the LUMO energies of the Cu-complexes (**1**-**2**). The HOMO orbital energy of the dGMP fragment is -3.66 eV and LUMO energies of the **1** and **2** are -3.26 eV and -3.65 eV respectively. Therefore the HOMO orbital energy of the dGMP fragment (-3.66 eV) is very close to the LUMO energy of **2** (-3.65 eV) than **1** (-3.26 eV). So the electron transfer from dGMP fragment to metal complexes is easier for **2** than **1**. Such finding agrees well with the experimental DNA binding constant of complexes **1** and **2**.

View Article Online
DOI: 10.1039/C5DT01471A



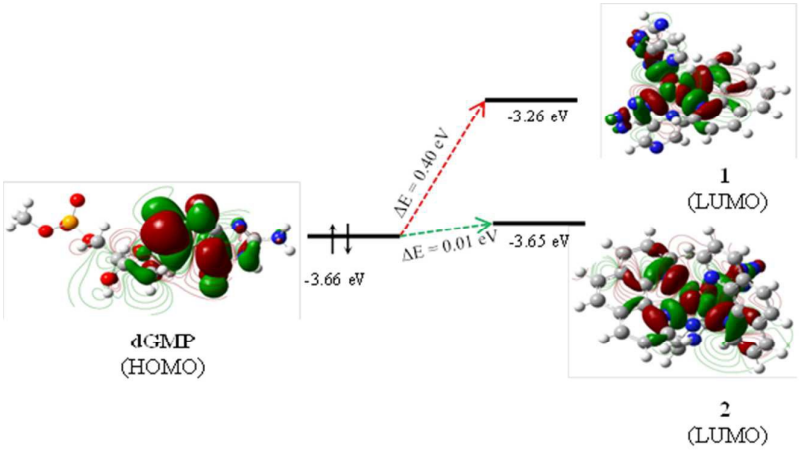


**Figure 6:** The position of the frontier orbitals of dGMP fragment and Cu-Complexes (**1** and **2**).

We have also modelled the complexes (**1** and **2**) bonded to the dGMP fragment (Figure 7). Here we consider, the dGMP fragment attacks the metal centre via the negatively charged O atom of the $PO_4^-$ group as shown in figure 7. Both the dGMP-bonded Cu-complexes are relaxed and found to be minima in their potential energy surfaces. We find the Cu-dGMP complex **2** is more distorted (Figure 7) than complex **1**. We have calculated the binding energy of the Cu complexes with dGMP fragments using the following equation.

$$E_B = E_{(Cu\text{-}dGMP)} - (E_{dGMP} + E_{Cu\text{-}complex})$$

The energy of the $E_{(Cu\text{-}dGMP)}$ is taken from the energy of the optimized structure of Cu- dGMP complex and the energy of the $E_{dGMP}$ and $E_{Cu\text{-}complex}$ are taken from the single point energy of the fragments within the geometry of the Cu-dGMP complex. Hence the single point energy is calculated by deleting the fragments one by one from the optimized geometry of the Cu-dGMP complexes.

The calculated binding energy between the dGMP and complex **1** and **2** are –0.59 Kcal/mol and –2.51 Kcal/mol respectively. Therefore the binding energy of the complexes (**1** and **2**) show similar trend as we found through our frontier orbitals study, which in turn agrees well with the experimental trend of the DNA binding constant.

View Article Online
DOI: 10.1039/C5DT01471A



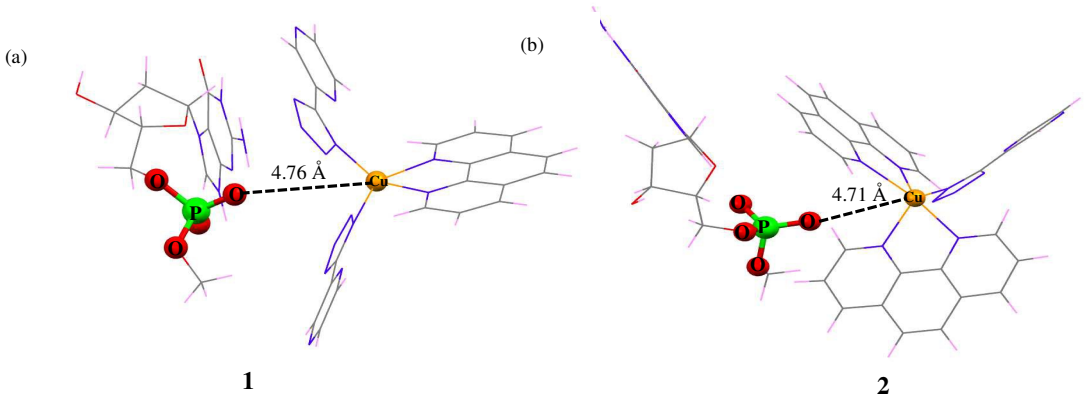


**Figure 7:** Optimized geometry of the Cu-dGMP complexes (**1** and **2**).

As both the complexes have shown considerable DNA binding ability therefore we started to explore the DNA cleavage activities for both the Cu tetrazolate complexes **1** and **2**. Plasmid pBR322 DNA was taken as the substrate in a medium of 50 mM Tris-HCl buffer (pH= 7.2) and the DNA cleavage activity was studied under physiological conditions. It is well known that circular plasmid DNA under conduction by electrophoresis splits into several bands. Fastest migration happens for supercoiled form (Form I). If one strand gets cleaved then nicked circular form is produced which moves in a slower manner with respect to supercoiled form (Form II). A linear form (Form III) is obtained when both strands are cleaved and it migrates between Form I and Form II.[42] Cleavage of supercoiled (SC) DNA (Form I) to nicked circular (NC) DNA (Form II) was observed for both the complexes by varying the concentration of the test solutions. The experiments were carried out in the concentration range of 50μM-400μM for the complexes **1** and **2** and the results obtained after 1 hour of incubation at a temperature of 40 °C are displayed in Figure 8a and Figure 8b respectively. Examination of these figures revealed that in control experiment no measurable DNA cleavage occurred when supercoiled pBR322 plasmid DNA was incubated whereas in presence of copper complex substantial cleavage of DNA was observed even in the absence of any co-reagents. This cleavage is more prominent in the case of complex **2** ( Figure 8b) where almost 91% of the DNA is cleaved to form nicked circular strands even in the absence of oxidizing agent $H_2O_2$ at 1μM concentration. With increasing concentration of copper complexes an enhanced DNA cleavage was observed. This cleavage may be due to the increased reaction of copper ions with $H_2O_2$, thereby producing diffusible hydroxyl radicals

View Article Online
DOI: 10.1039/C5DT01471A



or molecular oxygen, both of which are capable of damaging DNA by Fenton-type mechanism.[43] In the range of 50μM complex concentration, complex **2** possesses a superior DNA cleavage capability than complex **1** where the percentage of nicked circular is 46.2 for complex **1** (Table 5) and 94.8 in case of complex **2** (Table 6). It was also observed that higher concentration range of metal complexes **1** and **2**, promotes depletion of the supercoiled DNA form, with the consequent formation of linear DNA as a result of double stranded breaks. To explore the cleavage mechanism DNA cleavage was investigated with different potential radical scavangers to find out the intermediate which are possible reactive oxygen species (ROS) in presence and absence of external cofactors. DMSO and ethanol were used as a hydroxyl radical ($HO^{\cdot}$) scavenger and sodium azide was used as a singlet oxygen ($^1O_2$) scavenger and SOD was used as a Superoxide radical Scavenger. The results indicate that $NaN_3$ inhibits more than the other two scavengers to cleave DNA from SC form to NC form (Figure S15). This noticeable inhibition was observed with $NaN_3$, indicating the involvement of the Cu(II) complexes to cleave the SC form of pBR322 DNA by producing singlet molecular oxygen. [44]

The groove binding ability of complex **2** was studied in the presence of minor groove binder DAPI and major groove binder methyl green. As shown in figure S15, in presence of methyl green the band darkness for nicked circular DNA is very less. So it may be concluded that methyl green inhibits the cleavage of SC DNA to NC DNA, suggesting that the Cu complex **2** preferentially interacts through the major groove of the DNA helix.

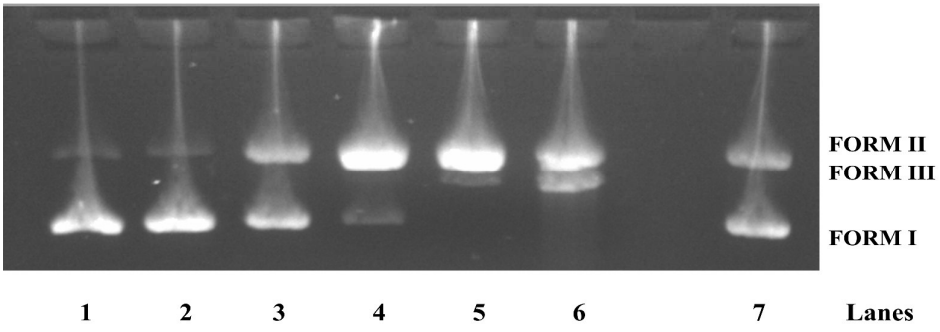


**Figure 8a:** Agarose gel electrophoresis cleavage showing cleavage of pBR322 supercoiled DNA by complex **1** after 1 hr of incubation at different concentration; Lane 1: DNA control; Lane 2: DNA+$H_2O_2$; Lane 3: DNA+$H_2O_2$+**1**(50μM); Lane 4: DNA+ $H_2O_2$+**1**(100μM); Lane 5: DNA+ $H_2O_2$+**1**(200μM); Lane 6 : DNA+ $H_2O_2$+**1**(400μM); Lane 7 : DNA+ **1**(50μM) .

View Article Online
DOI: 10.1039/C5DT01471A

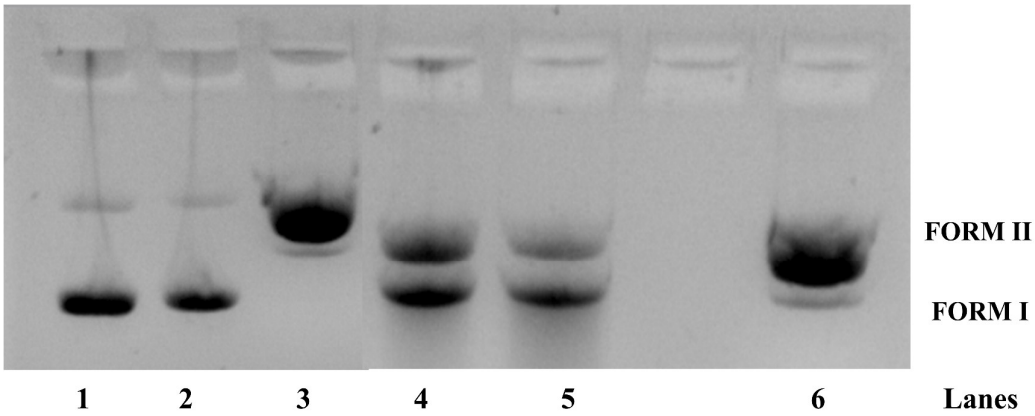


**Figure 8b:** Agarose gel electrophoresis cleavage showing cleavage of pBR322 supercoiled DNA by complex **2** after 1 hr of incubation at different concentration; Lane 1: DNA control; Lane 2: DNA+$H_2O_2$; Lane 3: DNA+$H_2O_2$+**2**(50µM); Lane 4: DNA+ $H_2O_2$+**2**(200µM); Lane 5: DNA+ $H_2O_2$+**2**(400µM); Lane 6 : DNA+ **2**(50µM) .

Interactions of bovine serum albumin (BSA) with copper complexes were studied through spectroscopic methods. It is well known that the interaction between metal complex and protein leads to the quenching of the fluorescence of the BSA protein and it may happen because of dynamic or static interaction.[45] In a dynamic mechanism the fluorescent molecule undergoes change only in the excited state whereas in a static quenching mechanism the interaction takes place at the ground state leading to considerable change in the absorption in UV-vis spectroscopy. The absorption peak for BSA is visible at 278 nm arising from the presence of aromatic amino acids (Trp, Tyr and Phe),[46] while with addition of both the complexes **1** and **2**, individually the absorption increases with a concomitant slight blue shift accompanied by it (Figure S16 and Figure S17). This is an indication of the interaction between BSA and the complex at ground state. This leads to conformational changes in BSA and induces a change in the polarity of the microenvironment around Tyr and Trp residues of BSA.[47]

View Article Online
DOI: 10.1039/C5DT01471A



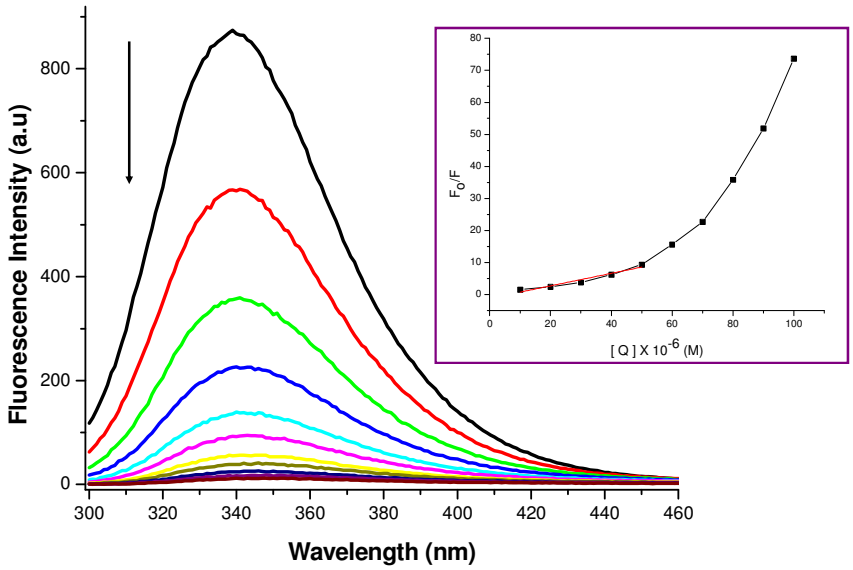


**Figure 9:** Fluorescence quenching of BSA by complex **1**. Stern–Volmer plot is in the inset.

To investigate further Trp-emission quenching experiments were carried out using BSA in the presence of increasing amounts of complexes **1** and **2**. A fixed amount of BSA solution was titrated with an increasing concentration of each complex. A continuous decrease of fluorescence intensity for the fluorophore was observed accompanied with a red shift (Figure 9 and Figure 10). The fluorescence emission was observed at 340 nm upon excitation at 290 nm. To get more insight concerning the interaction between complex and BSA the obtained result was analysed by the Stern-Volmer equation[48] :

$$\frac{F_0}{F} = 1 + k_q \tau_0 [Q] = 1 + K_{SV}[Q]$$

where $F_0$ and F are the fluorescence intensities in the absence and the presence of a quencher, $k_q$ is the bimolecular quenching rate constant, $\tau_0$ is the average lifetime of fluorophore in the absence of a quencher and [Q] is the concentration of a quencher (Metal complexes). In our case a non-linear plot with an increasingly upward trend was obtained (Figure 9 and Figure 10).

View Article Online
DOI: 10.1039/C5DT01471A

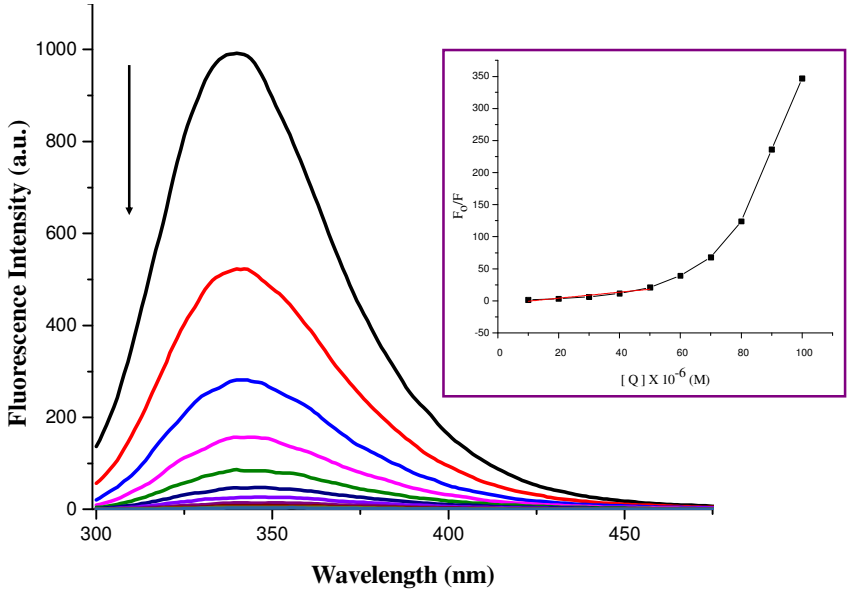


**Figure 10:** Fluorescence quenching of BSA by complex **2**. Stern–Volmer plot is in the inset.

This positive deviation indicates a probable two way quenching by collision and as well as by complex formation with the same quencher.[48] $K_{SV}$ is the Stern–Volmer quenching constant in $M^{-1}$ which can be determined by linear regression of $F_0/F$ against [Q]. The calculated value of the Stern–Volmer quenching constant ($K_{SV}$), the bimolecular quenching rate constant ($k_q$), and the number of binding sites (n) for both the complexes **1** and **2** are listed in Table 7. The values of the quenching constant from Stern–Volmer plot were found to be in the order of $10^{13}$. This value also indicates that there is a larger possibility that the quenching mechanism of fluorescence of BSA by two different complexes is initiated by static quenching process.[47] The binding constant value ($K_b$) and the number of binding sites (n) from Scatchard plot were obtained from the equation :

$$\log\left[\frac{F_0 - F}{F}\right] = \log K_a + n \log[Q]$$

The value of n was found to be more than 2 indicating that there might be two probable binding sites available in BSA for all the complexes (Figure S18 and Figure S19). The value of $K_b$ indicates a very strong interaction between copper complexes and BSA.

View Article Online
DOI: 10.1039/C5DT01471A



To explore the possible catecholase like activity of the copper complex 3,5-di-tert-butylcatechol (3,5-DTBC) was taken as the prospective substrate as the compound shows a low quinone-catechol reduction potential.[48] The reactions were carried out at 25°C in presence of air and monitoring was done by UV-vis spectroscopy. The experiments revealed that whereas complex **2** is quite active towards catalytic oxidation of 3,5-DTBC, complex **1** has not shown any such tendency. In case of complex **2** appearance of a new band at 440 nm occurred instantaneously upon addition of catechol which obscures the peak which is supposed to be observed at around 400 nm for the formation of benzoquinone. The peak observed at 440 nm may be attributed to ligand to metal charge transfer band because of the binding of phenoxo moiety to copper ion (Figure 11).[21] However, the reaction was monitored for 90 minutes and a hint of another peak gradually appears at 402 nm with time.

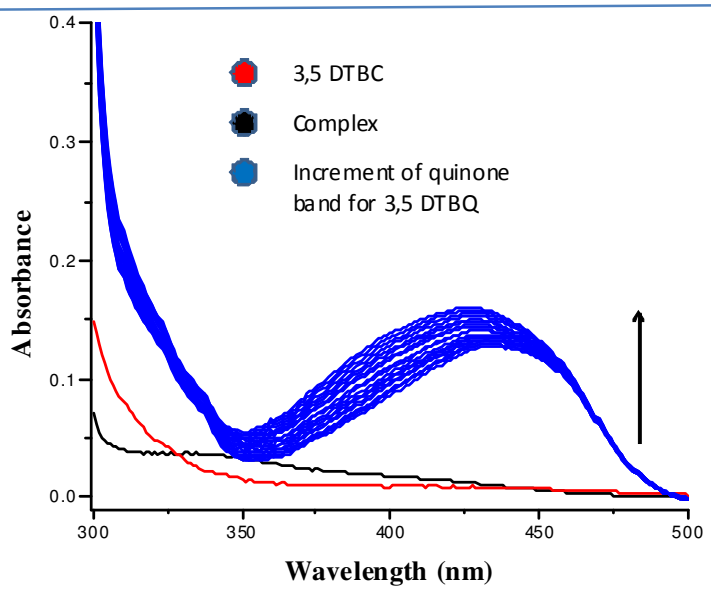


**Figure 11:** Spectral pattern of catecholase activity over time for complex **2** after addition of 3,5-DTBC.

To obtain the rate constant for the catalyst complex traditional initial rate method was employed and on the basis of the Michaelis–Menten approach of enzymatic kinetics, the observed rate versus substrate concentration data were then analyzed (Figure S20). Linearization of Lineweaver–Burk plot (Figure S20) provides the value of Michaelis–Menten constant ($K_M$) and maximum initial rate ($V_{max}$) which were found to be 0.00367 (M) and 0.0022 M $min^{-1}$. The turnover number values ($k_{cat}$) obtained was 1.32 X $10^4$ $h^{-1}$. These results clearly show the ability of complex **2** to effectively catalyse the oxidation of 3,5-DTBC . All the obtained kinetic parameters are presented in Table 8.

View Article Online
DOI: 10.1039/C5DT01471A



To look further into the probable mechanism, compound **2** was subjected to electrospray ionization mass spectrum in methanol solution which exhibits three assignable peaks at 570.45, 423.36 and 390.32 arising out of $[Cu(phen)_2(pzta)]^+$, $[Cu(phen)_2]^+$ (copper (II) gets reduced to copper (I) at ESI-mass spectroscopy condition) and $[Cu(phen)(pzta)]^+$ (Figure S2). To find out the possible complex-substrate intermediate ESI-MS positive spectrum was taken for a mixture of complex **2** and 3,5-DTBC in 1:100 molar ratio and recorded in 5 minutes interval. The spectra obtained was having lot of peaks indicating extensive fragmentation of the complex, substrate or complex-substrate intermediate. However, the peak at 243.1 is assigned as quinone-sodium aggregate $[(3,5\text{-DTBQ})Na]^+$. Among the remaining peaks the peak at 301.1 could be assigned for $\{[(phen)_2Cu\text{-}(OH)_2\text{-}Cu(phen)_2]^{2+} + Na^+\}$ and 339.2 could be for $[Cu(phen)_2(3,5\text{-DTBCH})(O_2)\text{-}H]^{2+}$ (Figure S21). Dimeric species similar to $[(phen)_2Cu\text{-}(OH)_2\text{-}Cu(phen)_2]^{2+}$ are also reported elsewhere as a probable intermediate for catcholase mimicking activity.[49] Identification of these two probable species helps us to understand and propose a possible mechanism for the catalytic process. To get further insight into the probable mechanism we have carried out qualitative as well as quantitative detection of $I_3^-$ band (~353nm) by UV-Vis spectroscopy for indication of formation of $H_2O_2$ during catalytic oxidation procedure. The experiment indicates the oxidation of $I^-$ to $I_2$ followed by the generation of $I_3^-$,which was qualitatively detected by UV-Vis spectral study of solution which is the outcome of the reduction of dioxygen to $H_2O_2$ as reported before (Figure S22).[48] Quantitative analysis of $H_2O_2$ indicates that 0.85 mol (≈1) of $H_2O_2$ was shown to be produced per mol of 3,5 DTBC along with formation of 1 mol 3,5 DTBQ, which strongly supports the mechanism of reaction involving a two electron reduction process of areal oxygen. Taking account of all the above experimental results a reaction mechanism is proposed (Scheme 2) in which the oxidation process occurs through catecholate bound copper(I) center (A) which gets generated by elimination of tetrazolate ion from the copper center and subsequent coordination by catechol in an unidentate manner keeping the option open for aerial oxygen to get attached to the copper(I) center to reoxidize it to copper (II) superoxide intermediate (B). The next step involves the intramolecular proton transfer process from oxygen atom of catechol moiety to the superoxide oxygen atom to produce a peroxo-intermediate (C) which upon reacting with moisture of the solvent molecule is generating the dihydroxo bridged copper (II) intermediate $[(bipy)_2Cu\text{-}(OH)_2\text{-}$

View Article Online
DOI: 10.1039/C5DT01471A



$Cu(bipy)_2]^{2+}$ (D) as evidenced by ESI-MS spectroscopy. Intermediate (D) upon further reaction with DTBC regenerates the copper (I) center (A) to complete the catalytic cycle.

## Conclusion

In conclusion two new octahedral water soluble copper complexes [Cu{(5-pyrazinyl)tetrazolate}$_2$(1,10-phenanthroline)] **1** and [Cu{(5-pyrazinyl)tetrazolate}(1,10-phenanthroline)$_2$]$(NO_3)_{0.5}(N_3)_{0.5}$ **2** were synthesized by [2 + 3] dipolar cycloaddition between copper ligated azide and pyrazinecarbonitrile. Single crystal X-ray diffraction (XRD) results for the complexes **1** and **2** revealed distorted octahedral geometry around the metal ion. Interaction with DNA and BSA binding studies of water soluble copper tetrazolate compounds have been explored. Both the complexes have shown binding ability to CT-DNA where compound **2** was found to be a stronger binder. DFT studies indicated that a lower HOMO-LUMO energy gap between DNA fragment and metal complexes might be the reason behind this kind of stronger interaction. Furthermore both the complexes **1** and **2** have shown DNA nuclease property in presence and absence of additional co-reagents. Inhibitation of DNA cleavage activity in presence of sodium azide indicates the involvement of singlet molecular oxygen in mechanistic pathway. The interaction of compound **1** and **2** with albumin protein show intense interaction between metal complex and protein with very high fluorescence quenching. The Stern–Volmer quenching constant value obtained was to the tune of $10^{13}$ $M^{-1}$ showing that both static and dynamic quenching occurring simultaneously. Apart from the above mentioned interaction with biomolecules complex **2** exhibited promising catecholase like activity with TON value to the order of $10^4$ $h^{-1}$. ESI-MS study indicates the mechanistic pathway of the reaction probably involves a dimeric copper intermediate $[(phen)_2Cu\text{-}(OH)_2\text{-}Cu(phen)_2]^{2+}$ as cited in various previous reports.

View Article Online
DOI: 10.1039/C5DT01471A



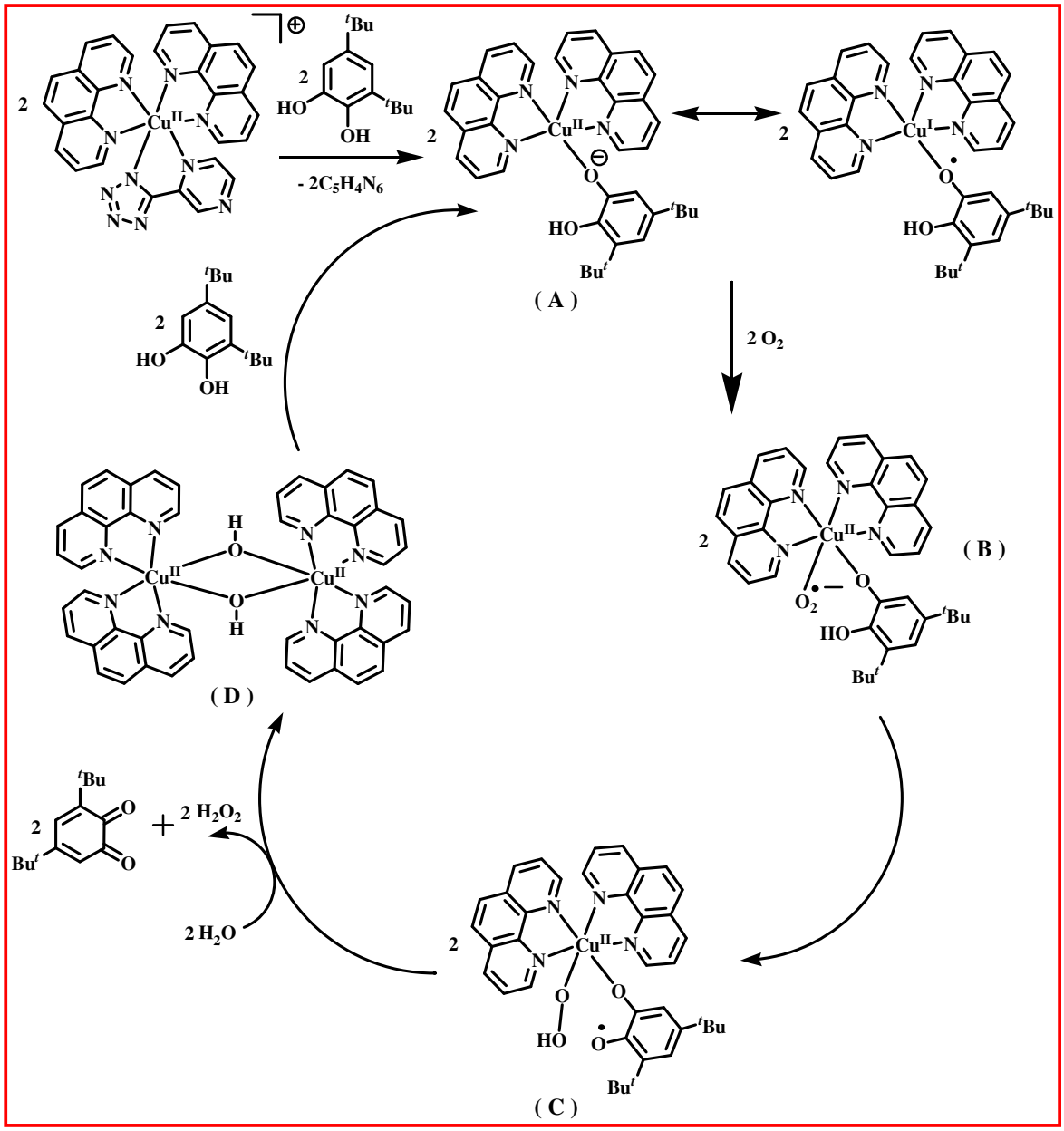


**Scheme 2: Probable catalytic cycle of oxidation of 3,5-DTBC by Cu(II) octahedral complex 2.**

View Article Online
DOI: 10.1039/C5DT01471A



## Experimental Section

### Materials and physical measurements

**Reagents and Materials.** All reagents and solvents were purchased commercially and were used as received. Copper(II) nitrate trihydrate, 1,10-phenanthroline monohydrate, sodium azide and pyrazine carbonitrile were purchased from Merck-India Chemical Company. Calf thymus DNA, bovine serum albumin (BSA, fraction V powder), ethidium bromide (EB), Agarose Low EEO Superior grade type II gel, supercoiled plasmid pBR322 DNA, DAPI dihydrochloride (4',6-diamidino-2-phenylindole dihydrochloride), methyl green and superoxide dismutase (SOD) were purchased from SRL (India). Tris(hydroxymethyl) aminomethane-hydrochloride (Tris-HCl) buffer was prepared using distilled water.

**Methods and Instrumentation.** Infrared spectra (4000 to 500 $cm^{-1}$) were recorded with a BRUKER TENSOR 27 instrument in KBr pellets. Mass spectrometric analyses were done on Bruker-Daltonics, microTOF-Q II mass spectrometer and elemental analyses were carried out with a Thermo Flash 2000 elemental analyzer. Spectrophotometric measurements were performed on a Varian UV-Vis spectrophotometer (Model: Cary100) (for absorption) and a Fluoromax-4p spectrofluorometer from Horiba JobinYvon (Model: FM-100) (for emission) using a quartz cuvette with path length of 1 cm.

**Caution!** *Azide and tetrazolate compounds are potentially explosive. Only a small amount of material should be prepared and handled with care.*

### X-ray crystallography

Single crystal X-ray structural studies of compound **1** and **2** were performed on a CCD Agilent Technologies (Oxford Diffraction) SUPER NOVA diffractometer. Data for both the complex **1** and **2** were collected at 150(2) K using graphite-monochromatic Mo $K_\alpha$ radiation ($\lambda_\alpha$ = 0.71073 Å) and Cu $K_\alpha$ radiation ($\lambda_\alpha$ = 1.54184 Å) respectively. The strategy for the data collection was evaluated using the CrysAlisPro CCD software. The data were collected by the standard phi-omega scan techniques and were scaled and reduced using the CrysAlisPro RED software. The structure was solved by direct methods using the SHELXS-97 and refined by full matrix least-squares with the SHELXL-97 for compound **1** and SHELX-2014 for compound **2**, refining on $F^2$. [50]

View Article Online
DOI: 10.1039/C5DT01471A



The positions of all the atoms were obtained by direct methods. All non-hydrogen atoms were refined anisotropically. The remaining hydrogen atoms were placed in geometrically constrained positions and refined with isotropic temperature factors, generally $1.2U_{eq}$ of their parent atoms. The contribution of solvent electron density was removed by the SQUEEZE routine in PLATON.[51]

**Synthesis.** $[Cu(phen)(N_3)_2]_n$ and $[Cu(phen)_2N_3](NO_3)\cdot(H_2O)$ was synthesized according to the literature procedure. [52, 53]

**Synthesis of $[Cu(phen)(pzta)_2]\cdot(H_2O)$ ($1\cdot H_2O$) and $[Cu(phen)_2(pzta)](NO_3)_{0.5}(N_3)_{0.5}\cdot 2(H_2O)$ ($2\cdot 2H_2O$) :**

A mixture of $[Cu(phen)(N_3)_2]_n$ (120 mg, 0.367 mmol), 2 mL of pyrazine carbonitrile and 3 mL of DMF was refluxed for 12 hrs . 30 mg of $NaNO_3$ was added and the reaction mixture was stirred for 30 mins at room temperature. The solvent was then removed in vacuo and the resulting residue was dissolved in methanol and filtered. The filtrate was concentrated to 2-3 ml. This greenish brown compound was found to be a mixture of two compounds *viz.* $[Cu(phen)(pzta)_2]$ and $[Cu(phen)_2(pzta)](NO_3)_{0.5}(N_3)_{0.5}$. The mixture was separated by ion-exchange chromatography using SP-Sephadex C-25, which is a strongly acidic ($-SO_3^-Na+$ ) cation exchanger based on cross-linked dextran. Methanol was used to elute the neutral complex $[Cu(phen)(pzta)_2]$ **1** and 0.1 M $NaNO_3$ solution was used as the elution solvent to run the column for the elution of the charged complex $[Cu(phen)_2(pzta)](NO_3)_{0.5}(N_3)_{0.5}$ **2**. Complex $\mathbf{1}\cdot H_2O$ was recrystallized from methanol–diethyl ether mixture to get suitable X-ray diffraction-quality crystals. Anal. Calc. for compound **1.$H_2O$**: $C_{44}H_{32}Cu_2N_{28}O_2$ (1112.02) : C 47.52; H 2.90; N 35.27%. Found: C 46.89; H 2.45; N 34.95%. ESI-MS (positive ion, $CH_3OH$) *m/z*: 537.7552 $[Cu(phen)(pzta)_2]^+$ (calcd 537.0822). IR ($cm^{-1}$, KBr): 3426, 1681,1642, 1523, 1023. Complex $\mathbf{2}\cdot 2H_2O$ was recrystallized from acetonitrile–diethyl ether mixture to get suitable X-ray diffraction-quality crystals. Anal. Calc. for compound $\mathbf{2}\cdot 2H_2O$ : $[C_{29}H_{19}N_{10}Cu](NO_3)_{0.5}(N_3)_{0.5}\cdot 2(H_2O)$ (659.13) : C 52.79; H 3.48; N 25.48%. Found: C 52.38; H 3.25; N 24.96%. ESI-MS (positive ion, $CH_3OH$) *m/z*: 570.1 $[M-NO_3]^+$ (calcd 570.109). IR ($cm^{-1}$, KBr, selected peak): 3414, 1624, 1385. IR ($cm^{-1}$, $CH_2Cl_2$, selected peak): 3424, 2111, 1628, 1377.

View Article Online
DOI: 10.1039/C5DT01471A



**Synthesis of exclusive $[Cu(phen)_2(pzta)](NO_3)_{0.5}(N_3)_{0.5}\cdot 2(H_2O)$ ($2\cdot 2H_2O$) :**

A mixture of $[Cu(phen)_2N_3](NO_3)\cdot(H_2O)$ (120 mg, 0.367 mmol), 2 mL of Pyrazine carbonitrile and 3 mL of DMF was refluxed for 12 hrs to get a clear green colour solution. The solvent was then removed in vacuo to obtain green colour residue upon concentration. This residue was dissolved in acetonitrile and layered with diethylether to obtain a relatively small amount of green coloured crystals, which were physically separated. Those crystals were then dissolved in acetonitrile and layered with ether. This procedure was repeated thrice to obtain an increasingly more pure compound **2** and the remaining mother solution was rejected. Anal. Calc. for compound $\mathbf{2}\cdot 2H_2O$ : $[C_{29}H_{19}N_{10}Cu](NO_3)_{0.5}(N_3)_{0.5}\cdot 2(H_2O)$ (659.13) : C 52.79; H 3.48; N 25.48%. Found: C 52.38; H 3.25; N 24.96%. ESI-MS (positive ion, $CH_3OH$) *m/z*: 570.1 $[M–NO_3]^+$ (calcd 570.109). IR ($cm^{-1}$, KBr, selected peak): 3414, 1624, 1385. IR ($cm^{-1}$, $CH_2Cl_2$, selected peak): 3424, 2111, 1628, 1377.

**Solubility and Stability.** The complexes are highly soluble in $H_2O$ and MeOH . They were stable in the solid and solution phases.

**DNA binding experiments.** The experiments involving the interaction of the complexes with calf thymus (CT) DNA were carried out in Tris-HCl buffer (50 mM Tris-HCl, pH 7.4). A solution of calf thymus DNA dissolved in this buffer gave a ratio of UV absorbance at 260 and 280 nm of about 1.8 : 1, suggesting the CT-DNA are sufficiently free from protein. The concentration of CT-DNA was estimated from its absorption intensity at 260 nm with a known molar extinction coefficient value (ε) of 6600 $M^{-1}cm^{-1}$ after 1 : 100 dilution. The stock solution of CT-DNA in buffer was stored at 4 °C and used within 4 days. Absorption titration experiments were carried out by varying the concentration of CT-DNA from 0-200μM while keeping the metal complex concentration constant at 10μM. Due correction were made for the absorbance of CT-DNA by adding an equal quantity of CT-DNA to both the complex solution and reference solution during titration. Moreover, DNA binding for both the complexes was measured by a special fluorescence spectral technique; ETBr displacement assay from ETBr bound CT-DNA in Tris-HCl buffer at biological pH 7.4. The fluorescence intensities of ethidium bromide (20 μM) at 605 nm (520 nm excitation) bound to DNA were measured with respect to concentration of the complex (0 to 100 μM). There was no apparent emission of Ethidium bromide in Tris-buffer medium (pH 7.4) because of fluorescence quenching of the free ethidium bromide by the solvent molecules. But in the presence of CT-

View Article Online
DOI: 10.1039/C5DT01471A



DNA, ethidium bromide shows appreciably improved emission intensity due to its intercalative binding to DNA. The competitive binding of the copper complexes to CT-DNA resulted the displacement of the bound EtBr which was manifested in decreasing its emission intensity.

**Interaction between DNA and complexes.** Absorption titration method has been used to monitor the mode of interaction of the complexes with CT-DNA. The intrinsic equilibrium DNA binding constants ($K_b$) of the complexes with DNA are determined by monitoring the change in the absorption intensity of the charge-transfer spectral bands of the compounds with increasing concentration of the DNA. In the experiment, there is addition of CT-DNA from 0-200 μM to the aqueous solution of complex **1**(12μM) and complex **2**(10μM) respectively. An intercalative binding of the complexes to DNA normally leads to hypochromism along with a bathochromic ( red) shift of the electronic spectral bands. From the changing tendency of UV spectras and the binding constants, we can conclude that the intercalative binding of complex **2** is more than complex **1**.

**BSA Interaction Studies.** The protein interaction study was performed by tryptophan fluorescence quenching experiments using BSA in TRIS-HCl buffer (pH ~ 7.4) with excitation at 295 nm and the corresponding emission at 340 nm, using a Fluoromax-4p spectrofluorometer [from Horiba JobinYvon (Model: FM-100)] with a rectangular quartz cuvette of 1 cm path length. Concentrated stock solutions of complexes **1** and **2** were prepared by dissolving them separately in TRIS-HCl buffer and diluted suitably with TRIS-HCl buffer to get the required concentrations. Quenching of the emission intensity of tryptophan residue of BSA (2 ml, 10μM) was monitored using complexes **1** and **2** (0-100 μM) as quenchers with increasing complex concentration. Furthermore, the interaction with proteins was also studied by measuring the increment in the absorption band at 278 nm in UV-Vis spectroscopy through successive addition of 0 to 100μM of complex **1** and **2** in 10 μM protein solution.

**Catecholase activity study :**.

In order to study the ability of the Cu(II) complexes to oxidize 3,5-DTBC, $2 \times 10^{-5}$ M methanolic solutions of complexes **1** and **2** were treated with $2 \times 10^{-3}$ M (100 equiv) of 3,5-DTBC under aerobic conditions at room temperature. In the UV−vis spectroscopy, where the absorbance of the resultant reaction mixture was plotted with respect to wavelength 300-500 nm, the time-dependent spectral scans for the complex **2** is plotted in Figure 11 . From the

View Article Online
DOI: 10.1039/C5DT01471A



figure, it is apparent that a band ~398 nm is observed to increase with time after the addition of 3,5-DTBC because of the gradual increment of the concentration of 3,5-DTBQ (3,5-DTBQ exhibits $\lambda_{max}$ ~ 400 nm in methanol) while no change is noticed in the spectral pattern with complex **1**. These data definitely reveal that complex **2** is an active catalysts for the aerial oxidation of 3,5-DTBC to 3,5-DTBQ, whereas complex **1** turns out to be inactive.

For the complex **2**, the kinetics for the oxidation of the substrate 3,5-DTBC was determined by the initial rate method at 25 °C. The substrate solutions of concentration ranging from 0.002 to 0.01 mol $dm^{-3}$ were prepared in methanol from a concentrated stock solution. A total of 2 mL of the substrate solution was poured into a 1 cm spectrophotometer quartz cell thermostatted at 25 °C. Then 1 mL of a 0.00002 M methanolic solution of complex **2** was quickly added to it so that the ultimate concentration of the complex became $1 \times 10^{-5}$ mol $dm^{-3}$. The dependence of the initial rate on the concentration of the substrate was spectrophotometrically monitored at the respective wavelength. Furthermore, the initial rate method display a first-order kinetics on the complex concentration and shows a saturation kinetics at higher substrate concentrations based on Michaelis–Menten model. The binding constant ($K_M$), maximum velocity (Vmax), and rate constant for dissociation of the substrates (i.e., turnover number, $k_{cat}$) were calculated for the complex **2** using the Lineweaver–Burk graph of 1/V versus 1/[S], (FigureS18) , with the equation $1/V = (K_M/V_{max})(1/[S]) + 1/V_{max}$, and all the obtained kinetic parameters are presented in table 8.

Iodometric method was followed to detect the formation of hydrogen peroxide during the catalytic reaction. The reaction mixtures were used as it was prepared in the kinetic experiments. After 45 mins of the reaction, an equal amount of water was added, to prevent further oxidation. Then the formed quinone was extracted three times with dichloromethane and the solution was acidified to pH = 2 with $H_2SO_4$. To the aqueous layer, 1 mL of 10% KI solution and two drops of 3% ammonium molybdate solution was added. The formation of $I_3^-$ was monitored by UV-Visible spectrophotometer due to the formation of the characteristic $I_3^-$ band at $\lambda$ = 353 nm. ( $\varepsilon$ = 14100 $M^{-1}$ $cm^{-1}$).



**Acknowledgement**

View Article Online
DOI: 10.1039/C5DT01471A

We are grateful for the financial support received from the Council of Scientific and Industrial Research, New Delhi. M. S. thanks CSIR for the award of SRF. We are also thankful Sophisticated Instrument Center, IIT Indore for the structure elucidation.

**Notes and references**

[a]*Department of Chemistry, School of Basic Sciences, Indian Institute of Technology Indore, IET-DAVV Campus, Khandwa Road, Indore 452017, India; Fax : (+91)-731-2361482; Tel: (+91)-731-2438705; E-mail : suman@iiti.ac.in*

[b]*University of North Texas at Dallas, Life and Health Sciences Department,7400 University Hills Blvd, 300 Founder's Hall, Dallas, TX 75241, USA. E-mail: myousuf@untdallas.edu*

[c] *Department of Applied Chemistry, Indian School of Mines, Dhanbad, 826004, Jharkhand, India, E-mail: hpnayek@yahoo.com*

† Electronic Supplementary Information (ESI) available: Cif files for the complexes **1** and **2′** and other necessary supplementary figures are provided. CCDC number: 1039303 ( for the normal structure ) and 1430170 (for the "squeezed" refined structure ) respectively.

References :

(1) Z.-J. Hou, Z.-Y. Liu, N. Liu, E.-C. Yang and X.-J. Zhao, *Dalton Trans.* 2015, **44,** 2223-2233.

(2) R. Nasani, M. Saha, S.M. Mobin, L. M. D. R. S. Martins, A.J.L. Pombeiro, A.M. Kirillov and S. Mukhopadhyay, *Dalton Trans.* 2014, **43,** 9944-9954.

(3) T. Pham, K.A. Forrest, A. Hogan, K. McLaughlin, J.L. Belof, J. Eckert and B. Space, *Journal of Materials Chemistry A: Materials for Energy and Sustainability* 2014, **2,** 2088-2100.

(4) I. Boldog, K. Domasevitch, J.K. Maclaren, C. Heering, G. Makhloufi and C.Janiak, *Cryst. Eng. Comm.* 2014, **16,** 148-151.

(5) L. Bergmann, J. Friedrichs, M. Mydlak, T. Baumann, M. Nieger and S. Bräse, *Chem. Commun.* 2013, **49,** 6501-6503.

View Article Online
DOI: 10.1039/C5DT01471A



(6) H.-F. Chen, W.-B. Yang, L. Lin, X.-G. Guo, X.-J. Dui, X.-Y. Wu, C.-Z. Lu and C.-J. Zhang, *Journal of Solid State Chemistry* 2013, **201,** 215-221.

(7) M. Wriedt, A.A. Yakovenko, G.J. Halder, A.V. Prosvirin, K.R. Dunbar and H.-C. Zhou, *J. Am. Chem. Soc.* 2013, **135,** 4040-4050.

(8) Dr. M. Wriedt, J.P. Sculley, A.A. Yakovenko, Dr. Y. Ma, Dr. G.J. Halder, Prof. Dr. P.B. Balbuena and Prof. Dr. H.-C. Zhou, *Angew. Chem., Int. Ed.* 2012, **51,** 9804-9808.

(9) P. Cui, L. Ren, Z. Chen, H. Hu, B. Zhao, W. Shi and P. Cheng, *Inorg. Chem.* 2012, **51,** 2303-2310.

(10) J.-Y. Wu, S.-M. Huang, Y.-C. Huang and K.-L. Lu, *Cryst. Eng. Comm*. 2012, **14,** 1189-1192.

(11) E.-C. Yang, Z.-Y. Liu, X.-Y. Wu, H. Chang, E.-C. Wang and X.-J. Zhao, *Dalton Trans.* 2011, **40,** 10082-10089.

(12) P. Pachfule, Y. Chen, S.C. Sahoo, J. Jiang and R. Banerjee, *Chem. Mater.* 2011, **23,** 2908-2916.

(13) X.-M. Zhang, J. Lv, F. Ji, H.-S. Wu, H. Jiao and P.V.R. Schleyer**,** *J. Am. Chem. Soc.* 2011, **133,** 4788-4790.

(14) (a) N. A. Daugherty and C. H. Brubaker Jr., *J. Am. Chem. Soc.* 1961, **83**, 3779–3782; (b) C.-Y. Liu, Y. Li, J.-Y. Ding, D.-W. Dong and F.-S. Han, *Chem.–Eur. J.* 2014, **20**, 2373; (c) B.G. Mukhopadhyay, S. Mukhopadhyay, M.F.C. Guedes da Silva, M.A.J. Charmier and A.J.L. Pombeiro, *Dalton Trans*. 2009, **24,** 4778-4785.

(15) A. Haleel, P. Arthi, N. Dastagiri Reddy, V. Veena, N. Sakthivel, Y. Arun, P.T. Perumald and A.K. Rahiman, *RSC Adv*. 2014, **4,** 60816–60830.

(16) B. Szafranowska and J. Beck, *Eur. J. Inorg. Chem.* 2013, **18,** 3167-3177.

(17) K. Darling, W. Ouellette and J. Zubieta, *Inorg. Chim. Acta*. 2012, **392,** 52-60.

(18) E.-C. Yang, Y. Feng, Z.-Y. Liu, T.-Y. Liu and X.-J. Zhao, *Cryst. Eng. Comm.*, 2011, **13,** 230-242 .

(19) H. Grove, J. Sletten, M. Julve, F. Lloret and J. J. Cano, *Chem. Soc., Dalton Trans.,* 2001, 259–265.

(20) M. Stylianou, C. Drouza, Z. Viskadourakis, J. Giapintzakis and A.D. Keramidas, *Dalton Trans.*, 2008, 6188–6204.

(21) M.C. Buzzeo, A.H. Iqbal, C.M. Long, D. Millar, S. Patel, M.A. Pellow, S.A. Saddoughi, A.L. Smenton, J.F.C. Turner, J.D. Wadhawan, R.G. Compton, J.A. Golen, A.L. Rheingold, and L.H. Doerrer, *Inorg. Chem*. 2004, **43,** 7709-7725.

View Article Online
DOI: 10.1039/C5DT01471A

(22) B.D. Wang, Z.Y. Yang and T.R. Li, *Bioorg. Med. Chem.* 2006, **14,** 6012–6021.

(23) B.D. Wang, Z.Y. Yang, P. Crewdson and D.Q. Wang, *J. Inorg. Biochem.* 2007, **101,** 1492–1504.

(24) T. Ma, J. Xu, Y. Wang, H. Yu, Y. Yang, Y. Liu, W. Ding, W. Zhu, R. Chen, Z. Ge, Y. Tan, L. Jia and T. Zhu, *J. Inorg. Biochem.* 2015, **144,** 38–46.

(25) A.K. Patra, S. Roy and A.R. Chakravarty, *Inorg. Chim. Acta* 2009, **362 ,** 1591–1599.

(26) B. Maity, M. Roy, B. Banik, R. Majumdar, R.R. Dighe and A.R. Chakravarty, *Organometallics* 2010, **29,** 3632–3641.

(27) K.M. Vyas, R.N. Jadeja, D. Patel, R.V. Devkar and V.K. Gupta, *Polyhedron* 2013, **65,** 262–274.

(28) T.F. Miao, J. Li, S. Li and N.L. Wang, *J. Phys. Chem. A,* 2014, **118,** 5692**–**5699.

(29) A.D. Becke, *Phys. Rev. A* 1988, **38,** 3098-3100.

(30) C. Lee, W. Yang and R.G. Parr, *Phys. Rev. B* 1988, **37,** 785-789.

(31) Gaussian 09, Revision D.01, M.J. Frisch, G.W. Trucks, H.B. Schlegel, G.E. Scuseria, M.A. Robb, J.R. Cheeseman, G. Scalmani, V. Barone, B. Mennucci, G.A. Petersson, H. Nakatsuji, M. Caricato, X. Li, H.P. Hratchian, A.F. Izmaylov, J. Bloino, G. Zheng, J.L. Sonnenberg, M. Hada, M. Ehara, K. Toyota, R. Fukuda, J. Hasegawa, M. Ishida, T. Nakajima, Y. Honda, O. Kitao, H. Nakai, T. Vreven, J.A. Montgomery, Jr., J.E. Peralta, F. Ogliaro, M. Bearpark, J.J. Heyd, E. Brothers, K. N. Kudin, V. N. Staroverov, R. Kobayashi, J. Normand, K. Raghavachari, A. Rendell, J. C. Burant, S. S. Iyengar, J. Tomasi, M. Cossi, N. Rega, J. M. Millam, M. Klene, J. E. Knox, J. B. Cross, V. Bakken, C. Adamo, J. Jaramillo, R. Gomperts, R. E. Stratmann, O. Yazyev, A. J. Austin, R. Cammi, C. Pomelli, J. W. Ochterski, R. L. Martin, K. Morokuma, V. G. Zakrzewski, G. A. Voth, P. Salvador, J. J. Dannenberg, S. Dapprich, A. D. Daniels, Ö. Farkas, J. B. Foresman, J. V. Ortiz, J. Cioslowski and D. Fox, *J. Gaussian, Inc.,* Wallingford CT, 2009.

(32) J. Tomasi, B. Mennucci and R. Cammi, *Chem. Rev*., 2005, **105,** 2999–3093.

(33) A. Dreuw and M. Head-Gordon, *J. Am. Chem. Soc.* 2004, **126,** 4007–4016.

View Article Online
DOI: 10.1039/C5DT01471A



(34) O. Gritsenko and E. J. Baerends, *J. Chem. Phys*. 2004, **121,** 655–660.

(35) S. Zalis, N. Ben-Amor and C. Daniel, *Inorg. Chem*. 2004, **43,** 7978–7985.

(36) S.P. Huang, Q.S. Zhang, Y. Shiota, T. Nakagawa, K. Kuwabara, K. Yoshizawa and C. Adachi, *J. Chem. Theory. Comput*. 2013, **9,** 3872–3777.

(37) I.A. Mikhailov, M.V. Bondar, K.D. Belfield and A.E. Masunov, *J. Phys. Chem. C.* 2009, **113,** 20719–20724.

(38) E. Stendardo, F.A. Ferrer, F. Santoro and R. Improta, *J. Chem. Theory. Comput*. 2012, **8,** 4483–4493.

(39) J. Preat, C. Michaux, D. Jacquemin and E.A. Perpete, *J. Phys. Chem. C*. 2009, **113,**16821–16833.

(40) X.W. Liu, J. Li, H. Deng, K.C. Zheng, Z.W. Mao and N.Ji. Liang, *Inorg. Chim. Acta.* 2005, **358,** 3311–3319.

(41) W.J. Mei, J. Liu, K.C. Zheng, L.J. Lin, H. Chao, A.X. Li, F.C. Yuna and L.N. Ji, *Dalton Trans.* 2003, 1352-1359.

(42) A. Jayamani, V. Thamilarasan, N. Sengottuvelan, P. Manisankar, S.K. Kang, Y.-I. Kim, and V. Ganesan, *Spectrochim. Acta. part A* 2014, **122,** 365-374.

(43) L. Li, K. Du, Y. Wang, H. Jia, X. Hou, H. Chao and L. Ji, *Dalton Trans*. 2013, **42** 11576-11588.

(44) J.H. Kwon, H.-J. Park, N. Chitrapriya, T.-S. Cho, S. Kim, J. Kim, I.H. Hwang, C. Kim, and S.K. Kim, *J. Inorg. Biochem.* 2014, **131,** 79–86.

(45) E. Sundaravadivel, S. Vedavalli, M. Kandaswamy, B. Varghese and P. Madankumar, *RSC adv.* 2014**, 4,** 40763-40775.

(46) D.J. Li, M. Zhu, C. Xu and B.M. Ji, *Eur. J. Med. Chem.* 2011, **46** , 588-599.

(47) T.H. Sanatkar, H. Hadadzadeh, Z. Jannesari, T. Khayamian, M. Ebrahimi, H.A. Rudbari, M. Torkzadeh-Mahani and M. Anjomshoa, *Inorg. Chim. Acta.* 2014, **423,** 256-272.

(48) M. Das, R. Nasani, M. Saha, S.M. Mobin and S. Mukhopadhyay, *Dalton Trans.*, 2015, **44,** 2299-2310.

(49) (a) R. Marion, N.M. Saleh, N.L. Poul, D. Floner, O. Lavastre and F. Geneste, *New J. Chem.* 2012, **36,** 1828-1835; (b) M. Kodera, T. Kawata, K. Kano, Y. Tachi, S. Itoh and S. Kojo, *Bull. Chem. Soc. Jpn*. 2003, **76,** 1957-1964.

View Article Online
DOI: 10.1039/C5DT01471A

(50) G. Sheldrick, Acta Crystallogr., Sect. A: Fundam. Crystallogr., 2008, **64,** 112–122.

(51) A. L. Spek, J. Appl. Crystallogr., 2003, **36,** 7–13.

(52) L. Li, Z. Jiang, D. Liao, S. Yan and G. Wang, *Transition Met. Chem.,* 2000, **25,** 630-634.

(53) S. Mistri, S. García-Granda, E. Zangrando and S.C. Manna, *Polyhedron* 2013, **50,** 333–338.

**Table 1 : Crystal Data and Structure Refinement of Complexes 1 and 2**

| | **1** | **2** [a] |
|---|---|---|
| Empirical formula | $C_{44}H_{32}Cu_2N_{28}O_2$ | $C_{29}H_{23}CuN_{12}O_{3.5}$ |
| Formula weight | 1112.02 | 659.13 |
| Wavelength(A) | 0.71073 | 1.54184 |
| Temperature(K) | 150(2) | 150(2) |
| Crystal system | Triclinic | Triclinic |
| Colour and shape | Blue block | Green block |
| Space group | P -1 | P-1 |
| a/Å | 12.3344(8) | 11.9248(10) |
| b/Å | 14.2954(9) | 11.9276(12) |
| c/Å | 15.4511(5) | 13.4576(11) |
| α/degree | 95.631(4) | 71.600(8) |
| β/degree | 107.583(4) | 68.381(8) |
| γ/degree | 108.242(6) | 70.668(8) |
| Volume($Å^3$) | 2410.1(2) | 1637.7(3) |
| Z | 2 | 2 |
| $D_{calcd}$/mg $m^{-3}$ | 1.527 | 1.337 |
| $\mu$(Mo Kα)/$mm^{-1}$ | 0.954 | 1.372 |
| F(000) | 1124 | 676 |
| Crystal size/mm | 0.33 x 0.26 x 0.21 | 0.210 x 0.180 x 0.130 |

View Article Online
DOI: 10.1039/C5DT01471A



| | | |
|---|---|---|
| θ range(°) | 2.96 to 25.00 | 3.622 to 71.321 |
| Limiting indices | -14<=h<=14<br>-16<=k<=16<br>-18<=l<=15 | -14<=h<=9<br>-14<=k<=13<br>-16<=l<=14 |
| Total/ unique no. of reflns. | 18321 / 8470 | 10588 / 6179 |
| $R_{int}$ | 0.0473 | 0.0275 |
| Data/restr./params. | 8470 / 0 / 685 | 6179 / 30 / 404 |
| GOF($F^2$) | 1.057 | 1.254 |
| R1, wR2 | 0.0442, 0.1054 | 0.0909, 0.2831 |
| R1, wR2 (all data) | 0.0593, 0.1198 | 0.0963, 0.2987 |
| Peak and hole (e $Å^{-3n}$) | 0.396 and -0.521 | 1.110 and -0.620 |

[a]The "SQUEEZE" program was applied to subtract the contribution of the disordered solvent from diffraction data of complex **2** (water molecules). Refinement was carried out after the solvent electron density was removed by the SQUEEZE routine in PLATON.

View Article Online
DOI: 10.1039/C5DT01471A



**Table 2: Selected bond lengths (Å) and bond angles (°) for Complex 1**

| | | | |
|---|---|---|---|
| Cu(1)-N(9) | 1.985(2) | N(9)-Cu(1)-N(2) | 167.25(11) |
| Cu(1)-N(2) | 2.012(2) | N(9)-Cu(1)-N(3) | 92.94(10) |
| Cu(1)-N(3) | 2.012(2) | N(2)-Cu(1)-N(3) | 95.04(10) |
| Cu(1)-N(1) | 2.037(2) | N(9)-Cu(1)-N(1) | 93.45(9) |
| Cu(1)-N(13) | 2.401(3) | N(2)-Cu(1)-N(1) | 81.68(9) |
| Cu(2)-N(23) | 1.991(3) | N(3)-Cu(1)-N(1) | 163.00(11) |
| Cu(2)-N(17) | 2.002(3) | N(9)-Cu(1)-N(13) | 74.80(10) |
| Cu(2)-N(16) | 2.022(3) | N(2)-Cu(1)-N(13) | 93.96(10) |
| Cu(2)-N(15) | 2.030(3) | N(3)-Cu(1)-N(13) | 100.43(10) |
| N(3)-N(4) | 1.347(3) | N(1)-Cu(1)-N(13) | 96.44(10) |
| N(4)-N(5) | 1.313(4) | N(23)-Cu(2)-N(17) | 93.24(12) |
| N(5)-N(6) | 1.342(4) | N(17)-Cu(2)-N(16) | 94.95(11) |

View Article Online
DOI: 10.1039/C5DT01471A



**Table 3: Selected bond lengths (Å) and bond angles (°) for Complex 2**

| | | | |
|---|---|---|---|
| Cu1-N5 | 2.003(4) | N5-Cu1-N9 | 70.9(1) |
| Cu1-N3 | 2.015(4) | N5-Cu1-N1 | 93.0(2) |
| Cu1-N1 | 2.026(3) | N3-Cu1-N1 | 171.2(2) |
| Cu1-N4 | 2.069(3) | N5-Cu1-N4 | 160.0(2) |
| Cu1-N2 | 2.231(4) | N3-Cu1-N4 | 80.9(2) |
| N(5)-N(6) | 1.312(5) | N1-Cu1-N4 | 94.9(2) |
| N(6)-N(7) | 1.302(7) | N5-Cu1-N2 | 99.8(1) |
| N(7)-N(8) | 1.335(8) | N3-Cu1-N2 | 94.7(1) |
| | | N1-Cu1-N2 | 78.2(1) |
| | | N(4)-Cu(1)-N(2) | 99.7(2) |

**Table 4: Absorption spectra peaks of compounds 1 and 2 in Methanol**

| **Compound no.** | **λ, nm (ε, $M^{-1}$ $cm^{-1}$ )** |
|---|---|
| **1** | 270 (72500) , 618 ( 38 ) |
| **2** | 269 (76500) , 669 ( 53.5 ) |

View Article Online
DOI: 10.1039/C5DT01471A



**Table 5: pBR322 SC DNA Cleavage Data for Complex 1**

| Serial No. | Reaction conditions | Form % | | |
|---|---|---|---|---|
| | | % Nicked Circular | % Supercoiled | % Linear |
| 1 | DNA Control | 5.3 | 94.7 | 0 |
| 2 | DNA+$H_2O_2$ | 5.5 | 94.5 | 0 |
| 3 | DNA+$H_2O_2$+**1**(50µM) | 46.2 | 53.8 | 0 |
| 4 | DNA+ $H_2O_2$+**1**(100µM) | 93.3 | 6.7 | 0 |
| 5 | DNA+ $H_2O_2$+**1**(200µM) | 94.5 | 0 | 5.5 |
| 6 | DNA+ $H_2O_2$+**1**(400µM) | 74.3 | 0 | 25.7 |
| 7 | DNA+ **1**(50µM) | 41.4 | 58.6 | 0 |

View Article Online
DOI: 10.1039/C5DT01471A



**Table 6: pBR322 SC DNA Cleavage Data for Complex 2**

| Serial No. | Reaction conditions | Form % | | |
|---|---|---|---|---|
| | | % Nicked Circular | % Supercoiled | % Linear |
| 1 | DNA Control | 8.9 | 91.1 | 0 |
| 2 | DNA+$H_2O_2$ | 7.3 | 92.7 | 0 |
| 3 | DNA+$H_2O_2$+**2**(50µM) | 94.8 | 0 | 5.2 |
| 4 | DNA+ $H_2O_2$+**2**(200µM) | 48.9 | 0 | 51.1 |
| 5 | DNA+ $H_2O_2$+**2**(400µM) | 34.5 | 0 | 65.5 |
| 6 | DNA+ **2**(50µM) | 91.4 | 0 | 8.6 |

**Table 7: Table for Stern–Volmer quenching constant, binding constant and binding site**

| System | $K_{SV}$ ($M^{-1}$) | $K_q$ ($M^{-1}$ $S^{-1}$) | $K_a$ ($M^{-1}$) | n |
|---|---|---|---|---|
| Complex **1**-BSA | 1.95 x $10^5$ | 3.155 x $10^{13}$ | 2.1647 x $10^{10}$ | 2.158 |
| Complex **2**-BSA | 4.62 x $10^5$ | 7.499 x $10^{13}$ | 6.1573 x $10^{12}$ | 2.623 |

**Table 8: Table for various kinetic parameters of catecholase activity**

| Complex /Catalyst | Fixed Complex/Catalyst Conc. (M) | $V_{max}$ (M $min^{-1}$) | Std. Error | $K_M$ (M) | Std. Error | $K_{cat}$ / T.O.N ($h^{-1}$) |
|---|---|---|---|---|---|---|
| Complex **2** | 0.00001 | 0.0022 | 5.022 X $10^{-4}$ | 0.00367 | 0.00133 | 1.32 x $10^4$ |

View Article Online
DOI: 10.1039/C5DT01471A



# Graphical abstract

## Targeted Water Soluble Copper-tetrazolate Complexes : Interactions with Biomolecules and Catecholase like Activities

Manideepa Saha,[a] Mriganka Das,[a] Rajendar Nasani,[a] Indrani Choudhuri,[a] Muhammed Yousufuddin,[b] Hari Pada Nayek,[c] Mobin M Shaikh,[a] Biswarup Pathak,[a] Suman Mukhopadhyay*[a]

Two new copper-tetrazolate complexes are synthesized by metal mediated [2 +3] cycloaddition reaction between copper bound azide and pyrazinecarbonitrile. Their interaction with DNA, bovine serum albumin (BSA) and catecholase like activity are explored. Interaction of the complexes with DNA are further investigated with density functional theory.